HHS Public Access

Author manuscript

J Cardiovasc Pharmacol Ther. Author manuscript; available in PMC 2015 August 10.

Published in final edited form as:

J Cardiovasc Pharmacol Ther. 2014 July ; 19(4): 368–381. doi:10.1177/1074248413520344.

Electrical Integration of Human Embryonic Stem Cell-Derived Cardiomyocytes in a Guinea Pig Chronic Infarct Model

Yuji Shiba[1,4,*], **Dominic Filice**[1,2,*], **Sarah Fernandes**[1,†,*], **Elina Minami**[3], **Sarah K. Dupras**[1], **Benjamin Van Biber**[1], **Peter Trinh**[1], **Yusuke Hirota**[4], **Joseph D. Gold**[5,6], **Mohan Viswanathan**[3], and **Michael A. Laflamme**[1]

[1]Department of Pathology, Center for Cardiovascular Biology, Institute for Stem Cell and Regenerative Medicine, University of Washington, Seattle, WA

[2]Department of Bioengineering, Center for Cardiovascular Biology, Institute for Stem Cell and Regenerative Medicine, University of Washington, Seattle, WA

[3]Department of Medicine/Cardiology, Center for Cardiovascular Biology, Institute for Stem Cell and Regenerative Medicine, University of Washington, Seattle, WA

[4]Department of Cardiovascular Medicine, Shinshu University, Matsumoto, Japan

[5]Geron Corporation, Menlo Park, CA

[6]Cardiovascular Institute, Stanford University, Stanford, CA

Abstract

Background—Human embryonic stem cell-derived cardiomyocytes (hESC-CMs) were recently shown to be capable of electromechanical integration following their direct injection into intact or recently injured guinea pig hearts, and hESC-CM transplantation in recently injured hearts correlated with improvements in contractile function and a reduction in the incidence of arrhythmias. The present study was aimed at determining the ability of hESC-CMs to integrate and modulate electrical stability following transplantation in a chronic model of cardiac injury.

Methods & Results—At 28 days following cardiac cryoinjury, guinea pigs underwent intra-cardiac injection of hESC-CMs, non-cardiac hESC-derivatives (non-CMs) or vehicle. Histology confirmed partial remuscularization of the infarct zone in hESC-CM recipients, while non-CM recipients showed heterogeneous xenografts. The three experimental groups showed no significant difference in the left ventricular dimensions or fractional shortening by echocardiography or in the incidence of spontaneous arrhythmias by telemetric monitoring. While recipients of hESC-CMs and vehicle showed a similar incidence of arrhythmias induced by programmed electrical stimulation at 4-weeks post-transplantation, non-CM recipients proved to be highly inducible, with

Correspondence to: Michael A. Laflamme, MD, PhD, Department of Pathology, Center for Cardiovascular Biology, Institute for Stem Cell and Regenerative Medicine, University of Washington, Brotman Building, Rm 442, 850 Republican St, Seattle, WA 98109, laflamme@u.washington.edu, Phone: 206-897-1518, Fax: 206-897-1540.

†Present address: Gilead Sciences, Fremont, CA

*These authors contributed equally to this study.

Disclosures

MAL is a scientific founder and equity holder in BEAT Biotherapeutics. JDG is a former employee and equity holder of Geron Corporation. This work was sponsored in part by a research agreement between Geron and the Laflamme laboratory.

a ~3-fold greater incidence of induced arrhythmias. In parallel studies, we investigated the ability of hESC-CMs to couple with host myocardium in chronically injured hearts by the intravital imaging of hESC-CM grafts that stably expressed a fluorescent reporter of graft activation, the genetically-encoded calcium sensor GCaMP3. In this work, we found that only ~38% (5 of 13) of recipients of GCaMP3+ hESC-CMs showed fluorescent transients that were coupled to the host electrocardiogram.

Conclusions—hESC-CMs engraft in chronically injured hearts without increasing the incidence of arrhythmias, but their electromechanical integration is more limited than was previously reported following their transplantation in a subacute injury model. Moreover, non-CM grafts may promote arrhythmias under certain conditions, a finding that underscores the need for input preparations of high cardiac purity.

Keywords

Human embryonic stem cell (hESC); cell transplantation; electrophysiology; cardiomyocyte

Introduction

Preclinical studies with human embryonic stem cell-derived cardiomyocytes (hESC-CMs) have provided exciting proof-of-concept for the use of these cells in cardiac repair [1–5], but concerns remain about their electrophysiological behavior in injured hearts [6–10]. Our group recently reported that hESC-CMs successfully engrafted following their direct injection into guinea pig hearts at 10 days following cardiac cryoinjury and that their transplantation resulted in improved contractile function and a reduction in spontaneous and induced arrhythmias relative to controls[11]. While the mechanistic basis for this anti-arrhythmic effect remains undetermined and its relevance to human or large animal models uncertain, it is consistent with prior observations in other systems, including transplantation studies with primary murine fetal cardiomyocytes injected into cryoinjured mouse hearts [12] and an in vitro arrythmogenic model involving the co-culture of hESC-CMs and rat neonatal cardiomyocytes[13].

Our group also used the guinea pig model to investigate whether hESC-CMs were capable of undergoing electromechanical integration with host myocardium following their transplantation in injured hearts. Although there was indirect evidence for their ability to couple with host cardiomyocytes following transplantation in uninjured hearts[14, 15], the healthy heart is a very different context from that of the injured heart, where both inflammation and fibrosis would be expected to function as barriers to host-graft integration. To resolve this uncertainty, we transplanted hESC-CMs that stably expressed the genetically-encoded fluorescent calcium sensor GCaMP3. GCaMP3+ hESC-CMs exhibit robust fluorescent transients with each contractile cycle, and this signal provides a convenient readout of graft activation. When we imaged GCaMP3+ hESC-CM grafts in uninjured guinea pig hearts, we found that the graft-derived fluorescent transients always occurred in a 1:1 relationship to the QRS complex of the host electrocardiogram (ECG), indicating seamless host-graft electromechanical integration[11]. On the other hand, when we imaged GCaMP3+ hESC-CM grafts transplanted into injured hearts, we observed 1:1 host-graft coupling in only ~60% of hearts, and many of the latter hearts contained both coupled

and uncoupled graft regions[11]. While this outcome indicates that we still have more work to do to optimize the integration of stem cell-derived grafts in recently injured hearts, intravital imaging of GCaMP3-expressing grafts provides a tool to assess host-graft integration and to test novel strategies to enhance this parameter.

Importantly, the aforementioned electrocardiographic and imaging studies were performed using a guinea pig model of *subacute* cardiac injury, i.e. in animals that underwent cell transplantation at 10 days post-injury. As such, these observations do not necessarily apply to outcomes following hESC-CM transplantation in chronically injured hearts with already established dysfunction and infarct scar tissue. Indeed, our group has already reported important differences in outcomes between these two contexts in the rat model: hESC-CM transplantation at 4 days post-injury mediated robust improvements in left ventricular dimensions and fractional shortening, but these beneficial effects were not observed following cell transplantation at 28 days post-injury[16]. Hence, we decided that it would be important to specifically revisit the electromechanical integration and ECG consequences of hESC-CM transplantation at a similarly late time-point in the more relevant guinea pig model, especially since this timing better reflects the end-stage heart failure patient population in which any novel hESC-derived therapy would likely be tested first.

Materials and Methods

Cell preparation

hESC-CMs were differentiated from the H7 hESC line, as previously described by our group [1, 17]. In brief, hESCs were expanded in the pluripotent state under feeder-free culture conditions, using either mouse embryonic fibroblast conditioned medium [18] or a defined, serum-free medium containing basic fibroblast growth factor and human transforming growth factor-β1 [19]. Cardiogenesis was then induced via the serial application of activin A and bone morphogenetic protein-4 (BMP4) under serum-free, monolayer culture conditions [1, 11, 17, 20]. To generate non-cardiac hESC derivatives, this same protocol was employed but without the addition of activin A and BMP4. Both hESC-CMs and non-cardiac derivatives were cultured for 15–17 days under differentiating conditions, followed by transient heat-shock, enzymatic harvest and cryopreservation as previously described[11, 17]. Immediately prior to cell transplantation, cryopreserved cells were thawed, rinsed and resuspended in a previously described pro-survival cocktail (PSC) that consisted of Matrigel supplemented with ZVAD (benzyloxycarbonyl-Val-Ala-Asp (O-methyl)-fluoromethyl ketone), Bcl-XL BH4 (cell-permeant TAT peptide), cyclosporine A, insulin-like growth factor-1 and pinacidil. Our group has previously shown that delivery in PSC enhances cell survival following intra-cardiac transplantation[1].

For experiments intended to assess the electromechanical integration of hESC-CMs in vivo, we used cardiomyocytes generated from transgenic H7 or RUES2 hESCs that stably express the calcium-sensitive fluorescent protein GCaMP3. These lines were created by the zinc finger nuclease-mediated insertion of a GCaMP3 expression cassette in the AAVS1 “safe-harbor” locus[11, 21, 22].

Surgical procedures

All studies were approved by the University of Washington Animal Care and Use Committee and conducted in accordance with federal guidelines. Figure 1A depicts the timeline for experiments intended to assess the consequences of hESC-CM transplantation on structure, contractile function and electrical stability in the guinea pig model of chronic cardiac injury. In brief, adult male guinea pigs underwent cardiac cryoinjury and placement of an implantable ECG transmitter (PhysioTel model CA-F40, Data Sciences International) as previously described[11]. 28 days later, animals underwent a second thoracotomy, and direct intra-cardiac injection of either PSC vehicle alone or 80×10^6 cells in a 150 μl volume of PSC. To prevent rejection of the xenografts, animals were treated with an immunosuppressive regimen of methylprednisolone and cyclosporine A from days −2 until euthanasia.

Figure 1B shows the timeline for parallel experiments intended to assess the electromechanical integration of hESC-CM grafts in vivo. For this, equivalent surgical procedures were used to induce cardiac cryoinjury, again followed by the transplantation of GCaMP3-expressing hESC-CMs at 28 days post-cryoinjury. At 14 days post-transplantation, animals were euthanized, and their hearts were rapidly excised for ex vivo imaging studies as described below.

Echocardiography

Left ventricular dimensions and fraction shortening were measured on days −2 and +28 relative to cell transplantation by transthoracic echocardiography (GE Vivid 7 ultrasound system outfitted with a 10 MHz pediatric transducer)[1, 11]. All echocardiographic scans and analyses were performed by an operator blinded to the experimental conditions.

Telemetric ECG recordings

ECG recordings were obtained in conscious, freely mobile animals at each of the following time points: at 6 hours post-cardiac injury; on days 1, 3, 7, 14, 21 and 27 post-injury; at 6 hours post-transplantation; on day +1 post-transplantation; and then every third day post-transplantation until euthanasia. A blinded cardiologist later analyzed the traces for the total number and frequency of events including single and multiform premature ventricular contractions (PVCs), as well as non-sustained (NSVT) and sustained ventricular tachycardia (SVT) as defined by Lambeth convention criteria [21].

Programmed electrical stimulation studies

Programmed electrical stimulation (PES) studies were performed as a terminal procedure on day +28 post-transplantation, using methods previously described by our group[11]. In brief, anesthetized and mechanically ventilated animals were outfitted for standard surface ECG recordings (PowerLab, ADInstruments), and a bipolar stimulating electrode was inserted across the diaphragm and onto the cardiac apex. Standard clinical PES protocols were then employed, including the application of single, double and triple extra-stimuli after a train of eight conditioning stimuli at a 200 ms cycle length. If no lethal arrhythmias were induced by extra-stimuli, we next applied burst pacing via three bursts of 100 consecutive stimuli at a

cycle length of 125 ms. Animals were then assessed a semiquantitative arrhythmia score after Shiba et al[11].

Intravital imaging studies

To assess the electromechanical integration of hESC-CMs in chronically injured hearts, intravital imaging of GCaMP3+ hESC-CM grafts was performed on day 14 post-transplantation[11]. For this, hearts were rapidly excised and maintained ex vivo by retrograde perfusion on a modified Langendorff apparatus. To remove potentially confounding motion artifacts and indirect graft activation through passive stretch, hearts were mechanically arrested by perfusion with either 2,3-butanedione monoxime (BDM) (n=9) or blebbistatin (n=4). Similar outcomes were observed with both mechanical uncouplers. Epicardial GCaMP3 fluorescent transients were then acquired using a previously described imaging system (Nikon SMZ100 epifluorescent stereomicroscope equipped with a high-speed Andor iXon 860 EM-CCD camera). The electrical activity of the isolated hearts was monitored by negative and positive leads placed on the base of the right ventricle and left ventricular apex. The presence and extent of host-graft coupling were then determined by correlating GCaMP3 fluorescent transients with the host ECG using custom Matlab scripts.

Histology

Hearts were evaluated by histochemical stains (hematoxylin-eosin, picrosirius red/fast green), immunostaining and in situ hybridization with a human-specific pan-centromeric probe, using methods previously detailed by our group [1, 23, 24]. Scar area was defined by picrosirius red-positive area, and wall thickness was measured at the midpoint of the scar area at the level of papillary muscles. The expansion index was calculated as follows[25]: expansion index= (LV cavity area/whole LV area)/relative scar thickness. For immunostaining, we used the primary antibodies against β-myosin heavy chain (clone A4.951), β3-tubulin (clone SDL.3D10), chromogranin A (clone LK2G10), connexin43 (rabbit polyclonal), embryonic skeletal myosin (clone F1.652), guinea pig CD45 (clone IH-1), human CD31 (clone JC70A), muscle creatine kinase (rabbit polyclonal), Oct4 (rabbit polyclonal), and pan-cytokeratins (clone AE1/AE3), as well as species-specific either biotinylated (Vector Labs) or fluorescent (Invitrogen/Molecular Probes) secondary antibodies. To highlight the boundaries between graft and non-graft cells, a subset of sections were counterstained with wheat germ agglutin, a lectin that binds cell membranes and matrix[26–29]. Histomorphometry was performed by a blinded observer using digitally-scanned brightfield images.

Results

Cardiac and non-cardiac hESC derivatives form stable grafts in chronically injured guinea pig hearts

Adult guinea pigs were subjected to direct cryoinjury of the anterior left ventricle via thoracotomy and were implanted with a subcutaneous telemetric electrocardiographic (ECG) transmitter. 28 days later, we used echocardiography to assess pre-transplantation mechanical function and then performed an intra-cardiac injection of either 80×10^6 H7 hESC-CMs in a pro-survival cocktail (PSC) of factors[1] previously shown to enhance hESC-

CM engraftment (n=15), 80×10^6 non-cardiac hESC-derivatives in PSC (n=15), or the PSC vehicle alone (n=16). The hESC-CM preparations employed had a mean cardiac purity of 69% (range 62–73%), as estimated by flow cytometry with an anti-α-actinin antibody. They did not include any detectable Oct4+ undifferentiated cells[11].

At 28 days post-transplantation (corresponding to 8-weeks post-cryoinjury), animals were euthanized, and their hearts were harvested to assess the extent of the scar, as well as the size, composition, and distribution of the graft. All animals showed transmural scar formation and thinning of the involved left ventricular free wall, and there was no significant difference in scar size or wall thickness between recipients of hESC-CMs, non-cardiac cells or PSC. The grafts in the recipients of hESC-CMs and non-cardiac derivatives measured 3.3±0.7% and 4.8±1.3% of the total scar area, respectively (p=0.72). All of the hESC-CM recipients showed partial remuscularization of the scarred zone by irregularly-contoured islands of human myocardium. This graft myocardium immunostained with the cardiac marker β-myosin heavy chain (β-MHC), and its human origin was confirmed by in situ hybridization with a human pan-centromeric probe (Figure 2A). The grafts expressed other expected cardiac markers, including muscle creatine kinase and sarcomeric actin (data not shown). Most of the graft myocardium was located within the central regions of the scar (as defined by picrosirius red staining), but we also found small myocardial implants in the peri-infarct (border) zone. Where present, these implants in the border zone showed occasional foci of host-graft contact and evidence of shared intercalated discs, as highlighted by immunostaining for the gap junction protein connexin-43 (Figure 2B).

One of the 15 hESC-CM recipients also showed rare microscopic aggregates of graft with cartilaginous differentiation, but no teratomas were found in these animals. In fact, 96.0±0.7% of the human nuclei could be accounted for by β-MHC immunohistochemistry, and the vast majority of the remaining non-cardiac cells had a fibroblastic morphology. The graft cells in hESC-CM recipients were uniformly negative for endothelial (anti-CD31), hematolymphoid (anti-CD45), neuronal (anti-β3-tubulin) and epithelial (anti-pan-cytokeratins) markers.

A comparable number of surviving human cells were found in the recipients of non-cardiac hESC-derivatives at 4-weeks post-transplantation (Figure 2C). These grafts did not include any β-MHC+ graft cardiomyocytes, but they did qualify as teratomas, as they included elements of all three embryonic germ layers. The majority of these graft cells had a fibroblastic morphology and failed to immunostain with any tested marker, but 21.0±6.1% immunostained positively with an epithelial marker (anti-pan-cytokeratins) and 1.6±0.3% with a skeletal muscle marker (anti-embryonic skeletal myosin). Only vanishing rare cells expressed neuronal (β3-tubulin) or neuroendocrine (chromogranin A) markers, and none expressed the endothelial cell marker CD31.

Transplantation of hESC-CMs had no effect on contractile function

By echocardiography, uninjured guinea pigs had a mean left ventricular end-diastolic dimension (LVDd) of 0.80±0.04 cm, a left ventricular end-systolic dimension (LVDs) of 0.52±0.03 cm, and a fractional shortening (FS) of 35.4±1.3% (n=5). Cryoinjured animals receiving PSC, non-cardiac hESC-derivatives, or hESC-CMs were examined by

echocardiography on day −2 and day +28 relative to cell transplantation, which corresponded to 4- and 8-weeks post-cryoinjury. As expected, by day −2, animals belonging to all three experimental groups showed similar increases in ventricular dimensions and a correspondingly reduced FS. Cell transplantation did not affect their subsequent contractile function: paired comparisons within each group revealed no significant change in LVDd, LVDs, or FS from day −2 to day +28 post-transplantation, nor were there significant differences in these parameters between groups on day +28 (Figure 3).

Transplantation of hESC-CMs had no effect on the incidence of spontaneous arrhythmias

At the time of cardiac cryoinjury, guinea pigs received a subcutaneous telemetric ECG transmitter [30, 31], and ambulatory ECG recordings were acquired at scheduled intervals from day −28 to day +28 relative to transplantation. Although we previously reported that uninjured control animals do not show spontaneous arrhythmias [11], cryoinjured animals did exhibit occasional events, including singlet and consecutive PVCs as well as rare episodes of NSVT and SVT. (See Figure 4A for representative examples of each.) As might be expected, the occurrence of arrhythmic events peaked shortly after cryoinjury but declined to a low level within a few days. A second spike of events was temporally associated with the repeat thoracotomy and cell transplantation (Figure 4B). Therefore, to avoid confounding our data with arrhythmias related to surgery rather than the engrafted cells, we focused on the monitoring period from day +3 to day +28 post-transplantation. Over this interval, we observed no statistically significant difference between the three groups in terms of either the number of arrhythmic events per hour or the fraction of animals exhibiting such events (Figure 4C).

Transplantation of hESC-CMs had no effect on the incidence of induced VT, but recipients of non-cardiac cells showed greater inducibility

To further evaluate the electrical stability of recipient hearts, all animals underwent in vivo electrophysiological testing via PES on day +28 post-transplantation. As might be expected given the late timepoint and the relatively low frequency of spontaneous events during ambulatory ECG monitoring, the cryoinjured guinea pig proved to be a fairly arrhythmia-resistant model with no episodes of spontaneous VT or VT induced by single or double extra-stimuli during PES studies. However, a small fraction of animals did show episodes of NSVT or SVT following triple extra-stimuli or, less commonly, burst pacing (see Figure 5A for representative traces). Importantly, when comparing hESC-CM recipients to PSC-only controls, we observed no difference in the incidence of induced VT or mean PES arrhythmia score (Figures 5B–D). On the other hand, the recipients of non-cardiac hESC-derivatives proved to be highly unstable, as evidenced by their approximately three-fold greater incidence of induced VT and correspondingly worse PES arrhythmia score.

Potential mechanisms for the increased susceptibility to arrhythmias in the recipients of non-cardiac hESC-derivatives

We next undertook studies to investigate the mechanism(s) responsible for the increased incidence of induced VT in the non-cardiac cell recipients. A number of possibilities could be eliminated based on our earlier observations. For instance, non-cardiac cell recipients did not differ from the other two experimental groups in terms of the extent of the scar, graft size

or global contractile function. Immune rejection can also be arrhythmogenic, so we considered the possibility that the non-cardiac hESC-derivatives evoked a more intense and therefore electrically irritating host immune reaction. However, immunohistochemistry with a guinea pig-specific pan-leukocyte antibody (CD45) revealed comparably mild cellular rejection in both non-cardiac cell and hESC-CM recipient hearts (data not shown).

The presence of significant numbers of electrically excitable cells and/or neuroendocrine cells releasing pro-excitatory factors (e.g. neurepinephrine) within the non-cardiac cell grafts could plausibly contribute to electrical instability. While this possibility cannot be completely excluded, it does seem unlikely: the non-cardiac cell grafts included only very rare skeletal muscle cells (Figure 6A), no chromogranin A-positive neuroendocrine cells (Figure 6B) and vanishingly rare β3-tubulin-positive neuronal cells (Figure 6C). Interestingly, a significant fraction of the non-cardiac graft did express connexin-43, a situation which has actually been associated with an arrhythmia-suppressive effect following the transplantation of other cell types[12, 32].

Finally, we also considered the possibility that the pro-arrhythmic effects of the non-cardiac cell grafts were mediated via an indirect, “paracrine” mechanism of action, i.e. a mechanism of action akin to the indirect effects of cell transplantation on contractile function [33]. While a detailed investigation of the indirect effects of cell transplantation on the electrophysiological properties of the recipient heart is beyond the scope of the present study, we hypothesized that the transplantation of non-cardiac hESC derivatives modulated the extent of autonomic innervation. The transplantation of other non-cardiac cell types has been reported to promote cardiac nerve sprouting [34], and such an effect could plausibly contribute to arrhythmias in the post-infarcted heart [35]. To investigate this, we used anti-β3-tubulin immunohistochemistry in combination with the human-specific in situ probe to identify *host* cardiac nerves. Consistent with our hypothesis, we found that the recipients of non-cardiac hESC-derivatives had significantly greater nerve ingrowth than did PSC or hESC-CM recipients (Figure 6D–G). We speculate that this effect may have been mediated in part by the release of nerve growth factor (NGF), which was present in medium conditioned by non-cardiac hESC-derivatives but not hESC-CMs (Figure 6H&I).

A subset of hESC-CM grafts in chronically injured hearts are coupled with host myocardium

To investigate the ability of hESC-CM grafts in injured hearts to couple with host myocardium, we conducted parallel experiments in which a separate cohort of animals (n=13) were transplanted with GCaMP3+ hESC-CMs at 28 days post-injury. We harvested their engrafted hearts at 14 days post-transplantation (corresponding to six weeks post-injury) and then performed intravital imaging during mechanical arrest ex vivo. We then correlated the timing of cyclic GCaMP3 fluorescent transients with QRS complexes of the host ECG and found that only 38% (5 of 13) of recipient hearts contained some regions of visible graft with 1:1 host-graft coupling (see Figures 7A–B and 7C–D for representative examples of hearts with either coupled or uncoupled GCaMP3+ hESC-CM graft tissue, respectively). Among these five hearts that had at least some regions of 1:1 coupled graft, four had coupled graft located within the injury scar, and the extent of coupled graft in these

varied considerably (Figure 7E–F). In two hearts, 100% of the visible graft area was coupled with the host ECG, while others had 94% and only 3% coupled graft. A fifth heart had hESC-CM graft located both within the injury scar and the viable host myocardium adjacent to the border zone; and, in this case, 1:1 coupled graft was limited to the latter area (accounting for 19% of the total graft footprint). During these imaging studies, the mean R-R interval of the host ECG measured 368 +/− 19 ms. Uncoupled graft regions fired rhythmically but varied widely in terms of their periodicity, and their activation did not occur in any obvious relationship to the host ECG (i.e. no 1:2, 1:3 or higher order coupling was detected). Finally, although these quantitative analyses were performed on mechanically arrested hearts, GCaMP3 hESC-CM grafts displayed qualitatively similar behavior prior to motion arrest.

Discussion

The successful development of cardiac therapies based on pluripotent stem cells will require the field to overcome a number of significant obstacles, including concerns about teratoma formation [36], immune rejection [37], and arrhythmias [6–9]. Here we report the first study to investigate the electromechanical integration and arrhythmogenic risk of hESC-CM transplantation using a chronic cardiac injury model. In this work, we found that hESC-CMs reliably formed small implants of human myocardium within the scarred injury zone but that this partial remuscularization was not accompanied by beneficial effects on contractile function. This negative outcome is consistent with our prior experience in the rat, in which the salutary effects of hESC-CM transplantation in a subacute infarct model did not translate to the chronically injured heart [16]. Similarly, while we previously found that hESC-CM transplantation mediated an intriguing arrhythmia-suppressive effect in the recently injured guinea pig heart[11], here we observed no difference in the incidence of spontaneous or induced arrhythmias between the chronically injured recipients of hESC-CMs or PSC vehicle alone.

Perhaps accounting in part for this lack of effect on contractile or electrophysiological endpoints, the successful engraftment and electromechanical integration of hESC-CM grafts in chronically injured guinea pig hearts was more limited than we had previously found to be the case for equivalent grafts in more recently injured hearts[11]. In this earlier work, we transplanted a comparable preparation of hESC-CMs at 10 days post-cryoinjury and found that surviving graft occupied 8.4±1.5% of the scar zone at 4 weeks post-transplantation. By contrast, in the present study, we found surviving hESC-CM graft occupied only 3.3±0.7% of the scar zone at this same time-point. Perhaps not surprisingly, these differences in graft size in subacute versus chronic injury models correlated with differences in the extent of electromechanical integration at 14 days post-transplantation. While we found approximately 60% (4 of 7) recipient hearts in the subacute model showed some amount of graft that was 1:1 coupled with host myocardium (with the area of coupled graft in those hearts ranging from 55 to 95%), here we found only 38% (5 of 13) of recipient hearts had 1:1 coupled graft (with the extent of coupled graft ranging from 3 to 100%). These were not matched, simultaneous experiments, so we cannot rule a contribution by subtle differences in cell preparation (e.g. dose of 80 versus 100 × 10^6 cells) or personnel, but it seems highly likely that the more hostile environment of the chronically injured was a major factor

underlying these divergent outcomes. Indeed, the chronically injured heart has a greater extent of fibrosis as well as already-established adverse remodeling and organ dysfunction, all of which would be expect to oppose the survival, integration and salutary effects of hESC-CM transplantation. While this reality underscores the critical need for new strategies to improve the electromechanical integration of hESC-CM grafts in the end-stage failing heart, our report does describe imaging tools and an animal model that should be useful in the testing of such interventions. Of course, it remains to be determined whether enhanced host-graft coupling will increase or decrease the incidence of arrhythmias.

An unexpected and potentially important finding in our study was the substantially higher incidence of induced arrhythmias in the recipients of non-cardiac hESC-derivatives. Importantly, this pro-arrhythmic effect occurred with non-cardiac grafts that lacked significant quantities of either electrically excitable or neuroendocrine cells, and it was not attributable to changes in infarct size, contractile function or immune rejection. By process of elimination, we concluded that the most likely explanation was an indirect, paracrine mechanism of action. We speculate that one contributor could be increased cardiac nerve ingrowth, perhaps mediated by graft release of NGF, but additional work (e.g. injection of graft cell conditioned medium) will be required to confirm this hypothesis. In any event, while much attention has been focused on cell transplantation and beneficial paracrine effects on mechanical function [33], our study suggests we should be mindful of potentially deleterious paracrine effects on cardiac electrophysiology.

A few important limitations to this study should be acknowledged. First, our experiments involved a relatively short duration of follow-up. Mummery and colleagues have pointed out the value of transplantation studies with longer endpoints; indeed, after transplanting hESC-CMs into acutely infarcted NOD-SCID mice, they observed beneficial effects on mechanical function at 4 weeks that disappeared by 12 weeks post-transplantation [38]. Our decision to limit the present study to 4 weeks post-transplantation (which corresponded to 8 weeks post-injury) reflects an attempt to balance practical considerations related to work in an immunocompetent host with the need for a suitably long ECG monitoring period. We reasoned that, since the baseline incidence of spontaneous infarct-related arrhythmias was already greatly reduced by 8 weeks post-injury, there would be little added value in exposing the animals to the risks of prolonged immunosuppression (e.g. increased xenograft rejection, opportunistic infections and/or chronic renal failure).

A second important caveat is that, while arguably a better model than the mouse or rat, there are obviously major differences in the size and sinus rate of the guinea pig heart versus that of the adult human. As such, we cannot rule out the possibility that graft-related arrhythmias will occur following hESC-CM transplantation in a larger, more relevant preclinical model or eventual human subjects. Indeed, preliminary data has been presented at a recent conference suggesting transient electrical instability followed hESC-CM transplantation in a primate infarct model[39]. Hence, rather than replacing the need for eventual safety studies in a large animal model, we regard the higher-throughput guinea pig model as a more suitable platform to test strategies to promote host-graft integration and screen for effects on electrical stability. Better integrated cardiomyocytes might show greater maturation and contribute more to force generation[40, 41], but they also might prove more arrhythmogenic.

We and others in the field are working to identify additional methods of enhancing graft size and integration, and the issue of graft-induced arrhythmias will likely need to be revisited if these efforts succeed. The model system described in this report would seem an appropriate and reasonably high-throughput platform in which to conduct such testing.

A third caveat is that, because the guinea pig has excellent collaterals and so is not amenable to the induction of myocardial infarction by coronary ligation[42], we instead performed direct cryoinjury of the left ventricular wall. Cryoinjury does have the advantage that it produces a very reproducible size and location of injury scar and so reduces animal-to-animal variability. On the other hand, because it results in the necrosis of all cell types, it may create a more hostile environment for cell engraftment than would be the case in an ischemia-reperfusion infarct model. If so, then our study may be best regarded as a worst-case scenario for hESC-CM engraftment and integration. We also recognize that there are important differences in the pathophysiology and timing of events following myocardial infarction and cryoinjury[43, 44], although these concerns were somewhat ameliorated by our study design, in particular, the use of chronically injured hearts in which wall thinning and ventricular dilatation was already well-established at the time of cell transplantation.

A final caveat is that, because GCaMP3 imaging and other structural and functional studies were conducted using two separate cohorts of animals, we cannot correlate the presence or extent of host-graft coupling with effects on contractile function or electrical stability. These experiments were done separately because the transgenic GCaMP3+ hESC line was not available at the time we commenced our initial transplantation studies in the chronic injury model. In principle, this correlation could be performed by repeating all of our echocardiographic and ECG experiments using GCaMP3+ hESC-CMs, although power calculations suggest that this would require an impractically large number of animals. At present, all that can be stated is that only a small minority of the hearts analyzed by these functional endpoints likely had large amounts of coupled graft. Note that our failure to observe effects on contractile function or electrical stability in this context is not suggestive of a large beneficial “paracrine” effect of hESC-CM transplantation in the absence of electromechanical integration.

Acknowledgments

We thank Luz Linares, Brian Johnson, Kara White, Wei-Zhong Zhu, Veronica Muskheli, Willimark Obenza and Jonathan Kim for expert technical assistance and Charles Murry for helpful scientific discussion. This work was supported by a grant from Geron Corporation, as well as by NIH grants R01-HL064387, K08-HL80431, and P01-HL094374 (to MAL). YS was supported in part by a fellowship awarded from the Banyu Life Science Foundation International.

References

1. Laflamme MA, Chen KY, Naumova AV, et al. Cardiomyocytes derived from human embryonic stem cells in pro-survival factors enhance function of infarcted rat hearts. Nat Biotechnol. 2007; 25:1015–1024. [PubMed: 17721512]
2. Caspi O, Huber I, Kehat I, et al. Transplantation of human embryonic stem cell-derived cardiomyocytes improves myocardial performance in infarcted rat hearts. J Am Coll Cardiol. 2007; 50:1884–1893. [PubMed: 17980256]

3. van Laake LW, Passier R, Monshouwer-Kloots J, et al. Human embryonic stem cell-derived cardiomyocytes survive and mature in the mouse heart and transiently improve function after myocardial infarction. Stem Cell Research. 2007; 1:9–24. [PubMed: 19383383]
4. Menard C, Hagege AA, Agbulut O, et al. Transplantation of cardiac-committed mouse embryonic stem cells to infarcted sheep myocardium: a preclinical study. Lancet. 2005; 366:1005–1012. [PubMed: 16168783]
5. Blin G, Nury D, Stefanovic S, et al. A purified population of multipotent cardiovascular progenitors derived from primate pluripotent stem cells engrafts in postmyocardial infarcted nonhuman primates. J Clin Invest. 2010; 120:1125–1139. [PubMed: 20335662]
6. Chen HS, Kim C, Mercola M. Electrophysiological challenges of cell-based myocardial repair. Circulation. 2009; 120:2496–2508. [PubMed: 20008740]
7. Gepstein L. Electrophysiologic implications of myocardial stem cell therapies. Heart Rhythm. 2008; 5:S48–52. [PubMed: 18456202]
8. Jonsson MK, Duker G, Tropp C, et al. Quantified proarrhythmic potential of selected human embryonic stem cell-derived cardiomyocytes. Stem Cell Res. 2010; 4:189–200. [PubMed: 20303332]
9. Liao SY, Liu Y, Siu CW, et al. Proarrhythmic risk of embryonic stem cell-derived cardiomyocyte transplantation in infarcted myocardium. Heart Rhythm. 2010; 7:1852–1859. [PubMed: 20833268]
10. Zhang YM, Hartzell C, Narlow M, Dudley SC Jr. Stem cell-derived cardiomyocytes demonstrate arrhythmic potential. Circulation. 2002; 106:1294–1299. [PubMed: 12208808]
11. Shiba Y, Fernandes S, Zhu WZ, et al. Human ES-cell-derived cardiomyocytes electrically couple and suppress arrhythmias in injured hearts. Nature. 2012; 489:322–325. [PubMed: 22864415]
12. Roell W, Lewalter T, Sasse P, et al. Engraftment of connexin 43-expressing cells prevents post-infarct arrhythmia. Nature. 2007; 450:819–824. [PubMed: 18064002]
13. Thompson SA, Burridge PW, Lipke EA, Shamblott M, Zambidis ET, Tung L. Engraftment of human embryonic stem cell derived cardiomyocytes improves conduction in an arrhythmogenic in vitro model. J Mol Cell Cardiol. 2012; 53:15–23. [PubMed: 22713758]
14. Kehat I, Khimovich L, Caspi O, et al. Electromechanical integration of cardiomyocytes derived from human embryonic stem cells. Nat Biotechnol. 2004; 22:1282–1289. [PubMed: 15448703]
15. Xue T, Cho HC, Akar FG, et al. Functional integration of electrically active cardiac derivatives from genetically engineered human embryonic stem cells with quiescent recipient ventricular cardiomyocytes: insights into the development of cell-based pacemakers. Circulation. 2005; 111:11–20. [PubMed: 15611367]
16. Fernandes S, Naumova AV, Zhu WZ, Laflamme MA, Gold J, Murry CE. Human embryonic stem cell-derived cardiomyocytes engraft but do not alter cardiac remodeling after chronic infarction in rats. J Mol Cell Cardiol. 2010; 49:941–949. [PubMed: 20854826]
17. Xu C, Police S, Hassanipour M, et al. Efficient generation and cryopreservation of cardiomyocytes from human embryonic stem cells. Regen Med. 2011:6.
18. Xu C, Inokuma MS, Denham J, et al. Feeder-free growth of undifferentiated human embryonic stem cells. Nat Biotechnol. 2001; 19:971–974. [PubMed: 11581665]
19. Li Y, Powell S, Brunette E, Lebkowski J, Mandalam R. Expansion of human embryonic stem cells in defined serum-free medium devoid of animal-derived products. Biotechnol Bioeng. 2005; 91:688–698. [PubMed: 15971228]
20. Zhu WZ, Van Biber B, Laflamme MA. Methods for the derivation and use of cardiomyocytes from human pluripotent stem cells. Methods Mol Biol. 2011; 767:419–431. [PubMed: 21822893]
21. Walker MJ, Curtis MJ, Hearse DJ, et al. The Lambeth Conventions: guidelines for the study of arrhythmias in ischaemia infarction, and reperfusion. Cardiovasc Res. 1988; 22:447–455. [PubMed: 3252968]
22. Hockemeyer D, Soldner F, Beard C, et al. Efficient targeting of expressed and silent genes in human ESCs and iPSCs using zinc-finger nucleases. Nat Biotechnol. 2009; 27:851–857. [PubMed: 19680244]
23. Laflamme MA, Gold J, Xu C, et al. Formation of human myocardium in the rat heart from human embryonic stem cells. Am J Pathol. 2005; 167:663–671. [PubMed: 16127147]

24. Fernandes S, Naumova AV, Zhu WZ, Laflamme MA, Gold J, Murry CE. Human embryonic stem cell-derived cardiomyocytes engraft but do not alter cardiac remodeling after chronic infarction in rats. J Mol Cell Cardiol. 2010
25. Dvir T, Kedem A, Ruvinov E, et al. Prevascularization of cardiac patch on the omentum improves its therapeutic outcome. Proc Natl Acad Sci U S A. 2009; 106:14990–14995. [PubMed: 19706385]
26. Ang KL, Shenje LT, Reuter S, et al. Limitations of conventional approaches to identify myocyte nuclei in histologic sections of the heart. Am J Physiol Cell Physiol. 2010; 298:C1603–1609. [PubMed: 20457832]
27. Nizheradze KA. Binding of wheat germ agglutinin to extracellular network produced by cultured human fibroblasts. Folia Histochem Cytobiol. 2000; 38:167–173. [PubMed: 11185721]
28. Ohno J, Tajima Y, Utsumi N. Binding of wheat germ agglutinin in the matrix of rat tracheal cartilage. Histochem J. 1986; 18:537–540. [PubMed: 3804790]
29. van Laake LW, van Donselaar EG, Monshouwer-Kloots J, et al. Extracellular matrix formation after transplantation of human embryonic stem cell-derived cardiomyocytes. Cell Mol Life Sci. 2010; 67:277–290. [PubMed: 19844658]
30. Shiotani M, Harada T, Abe J, Hamada Y, Horii I. Methodological validation of an existing telemetry system for QT evaluation in conscious guinea pigs. J Pharmacol Toxicol Methods. 2007; 55:27–34. [PubMed: 16831559]
31. Shiotani M, Harada T, Abe J, et al. Practical application of guinea pig telemetry system for QT evaluation. J Toxicol Sci. 2005; 30:239–247. [PubMed: 16141657]
32. Mills WR, Mal N, Kiedrowski MJ, et al. Stem cell therapy enhances electrical viability in myocardial infarction. J Mol Cell Cardiol. 2007; 42:304–314. [PubMed: 17070540]
33. Gnecchi M, Zhang Z, Ni A, Dzau VJ. Paracrine mechanisms in adult stem cell signaling and therapy. Circ Res. 2008; 103:1204–1219. [PubMed: 19028920]
34. Pak HN, Qayyum M, Kim DT, et al. Mesenchymal stem cell injection induces cardiac nerve sprouting and increased tenascin expression in a Swine model of myocardial infarction. J Cardiovasc Electrophysiol. 2003; 14:841–848. [PubMed: 12890047]
35. Ieda M, Kimura K, Kanazawa H, Fukuda K. Regulation of cardiac nerves: a new paradigm in the management of sudden cardiac death? Curr Med Chem. 2008; 15:1731–1736. [PubMed: 18673222]
36. Nussbaum J, Minami E, Laflamme MA, et al. Transplantation of undifferentiated murine embryonic stem cells in the heart: teratoma formation and immune response. Faseb J. 2007; 21:1345–1357. [PubMed: 17284483]
37. Swijnenburg RJ, Schrepfer S, Cao F, et al. In vivo imaging of embryonic stem cells reveals patterns of survival and immune rejection following transplantation. Stem Cells Dev. 2008; 17:1023–1029. [PubMed: 18491958]
38. van Laake LW, Passier R, Doevendans PA, Mummery CL. Human embryonic stem cell-derived cardiomyocytes and cardiac repair in rodents. Circ Res. 2008; 102:1008–1010. [PubMed: 18436793]
39. Christoffels VM, Pu WT. Developing insights into cardiac regeneration. Development. 2013; 140:3933–3937. [PubMed: 24046314]
40. Halbach M, Pfannkuche K, Pillekamp F, et al. Electrophysiological maturation and integration of murine fetal cardiomyocytes after transplantation. Circ Res. 2007; 101:484–492. [PubMed: 17641227]
41. Pillekamp F, Reppel M, Rubenchyk O, et al. Force measurements of human embryonic stem cell-derived cardiomyocytes in an in vitro transplantation model. Stem Cells. 2007; 25:174–180. [PubMed: 16973834]
42. Maxwell MP, Hearse DJ, Yellon DM. Species variation in the coronary collateral circulation during regional myocardial ischaemia: a critical determinant of the rate of evolution and extent of myocardial infarction. Cardiovasc Res. 1987; 21:737–746. [PubMed: 3440266]
43. van den Bos EJ, Mees BM, de Waard MC, de Crom R, Duncker DJ. A novel model of cryoinjury-induced myocardial infarction in the mouse: a comparison with coronary artery ligation. Am J Physiol Heart Circ Physiol. 2005; 289:H1291–1300. [PubMed: 15863462]

44. Ciulla MM, Paliotti R, Ferrero S, et al. Left ventricular remodeling after experimental myocardial cryoinjury in rats. J Surg Res. 2004; 116:91–97. [PubMed: 14732353]

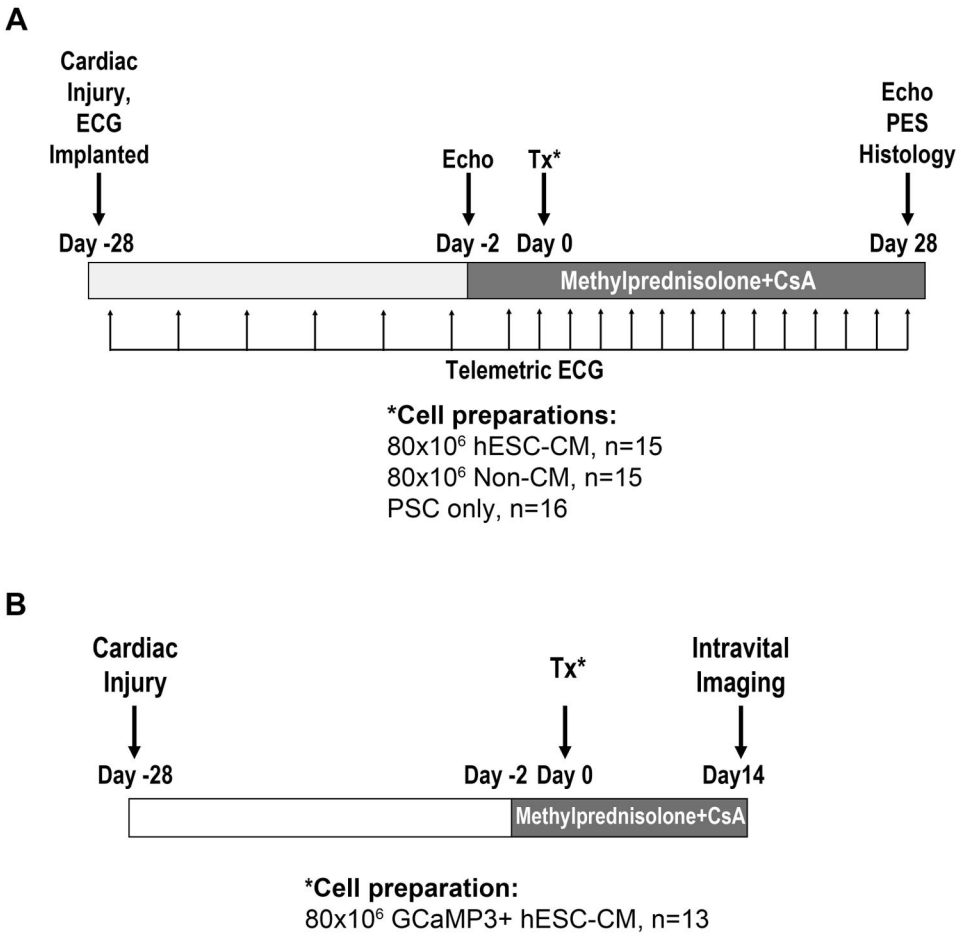

Figure 1. Experimental design

(A) To determine the structural and functional consequences of hESC-CM transplantation in a chronic injury model, guinea pigs underwent direct cryoinjury of the left ventricle and implantation with a telemetric ECG transmitter. 28 days later, they received an intra-cardiac injection of either hESC-CMs in pro-survival cocktail (PSC)[1], non-cardiac hESC derivatives in PSC, or the PSC vehicle alone. Endpoints included histology (on day +28 post-transplantation), echocardiography (performed on days −2 and +28 relative to transplantation), spontaneous arrhythmias by telemetric ECG (performed at the indicated time points), and induced arrhythmias by programmed electrical stimulation (PES, performed on day +28 post-transplantation). **(B)** To assess the electromechanical integration of hESC-CM grafts in this same chronic model, guinea pigs were injected with GCaMP3+ hESC-CMs in PSC at 28 days post-injury, followed by intravital imaging of engrafted hearts at 14 days post-transplantation. CsA, cyclosporine.

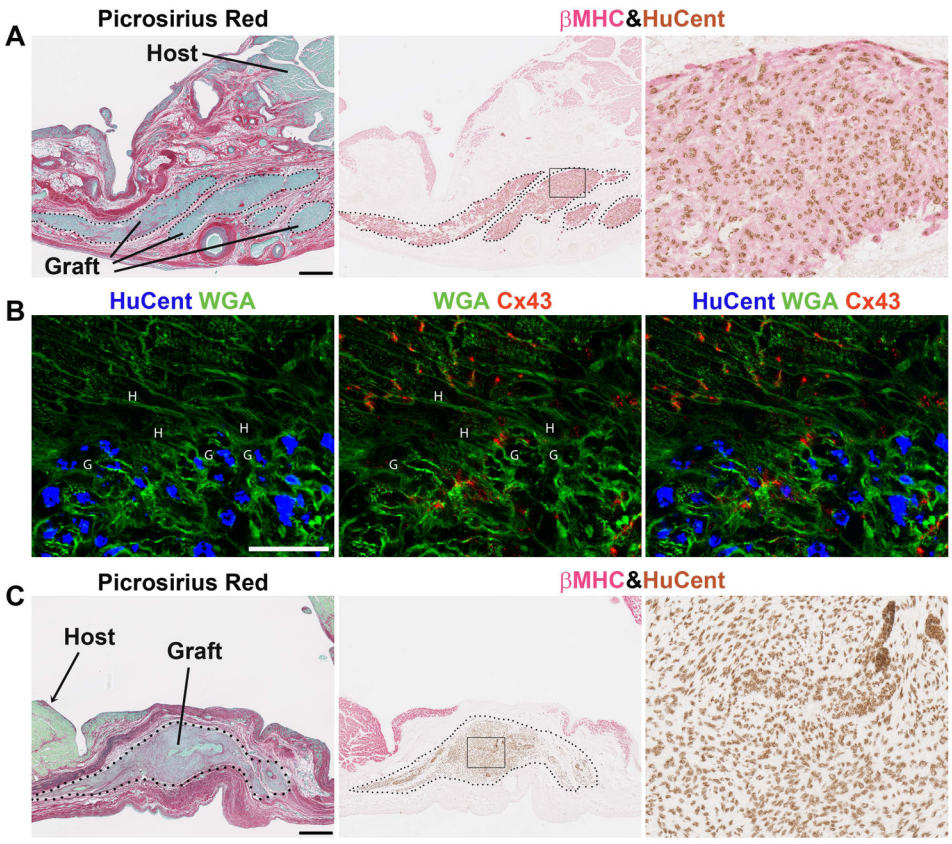

Figure 2. hESC-derived cardiac and non-cardiac grafts survive in chronically injured guinea pig hearts

Histological evaluation of hearts on day +28 post-transplantation. **(A)** Representative photomicrographs from an hESC-CM recipient demonstrating substantial implants of human myocardium within the scar tissue. By picrosirius red stain (left panel), the scar appears red and viable tissue green. The human origin of the graft myocardium was confirmed by combined in situ hybridization with a human-specific pan-centromeric (HuCent, brown) probe and β-myosin heavy chain (βMHC, red) immunohistochemistry (middle panel and inset to the right). **(B)** Confocal image of host-graft contact, labeled with HuCent (blue nuclei), wheat germ agglutinin (WGA, green), and connexin43 (Cx43, red). The letters H and G in the figure indicate host and graft cardiomyocytes, respectively. **(C)** Recipients of non-cardiac hESC-derivatives also showed surviving human graft within the scarred zone, but this human graft was negative for cardiac markers including βMHC. Scale bars=500 μm.

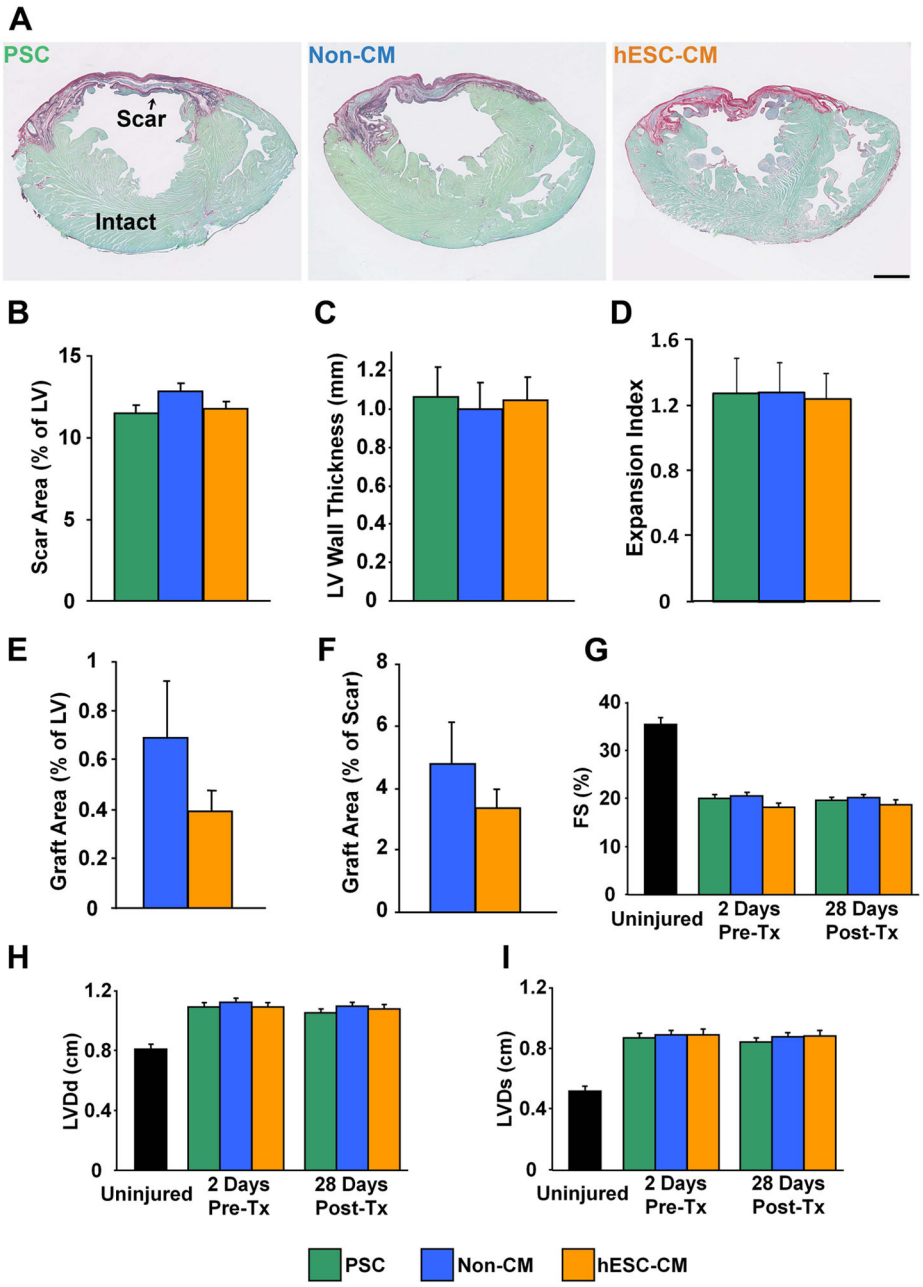

Figure 3. hESC-CM recipients and controls showed no significant differences in LV structure or function

(A–F). Histomorphometry of engrafted hearts on day +28 post-transplantation. **(A)** Representative picrosirius red/fast green-stained histological sections from recipients of the pro-survival cocktail (PSC, green, n=16), non-cardiac hESC-derivatives (Non-CM, blue, n=15), and hESC-CMs (orange, n=15). Scale bar=2 mm. The three experimental groups showed no significant difference in the extent of the scar area **(B**, expressed as the percentage of left ventricular wall cross-sectional area occupied as defined by picrosirius red-positive scar), wall thickness (**C**, measured at the midpoint of the scar area at the level of papillary muscles), or expansion index (**D**). Similarly, the groups showed no difference in

graft size, whether expressed as a percentage of total left ventricular (**E**) or scar (**F**) area. For the latter determination, grafts were identified by in situ hybridization with a human-specific pan-centromeric probe. **(F–H)** These same animals were analyzed by echocardiography on days −2 and +28 relative to transplantation. No significant difference was in left ventricular diastolic dimension (**F**, LVDd), left ventricular systolic dimension (**G**, LVDs), and fractional shortening (**H**, FS), either between the three experimental groups or between time points within each group. Black bars indicate corresponding values for these echocardiographic parameters in uninjured, non-engrafted hearts.

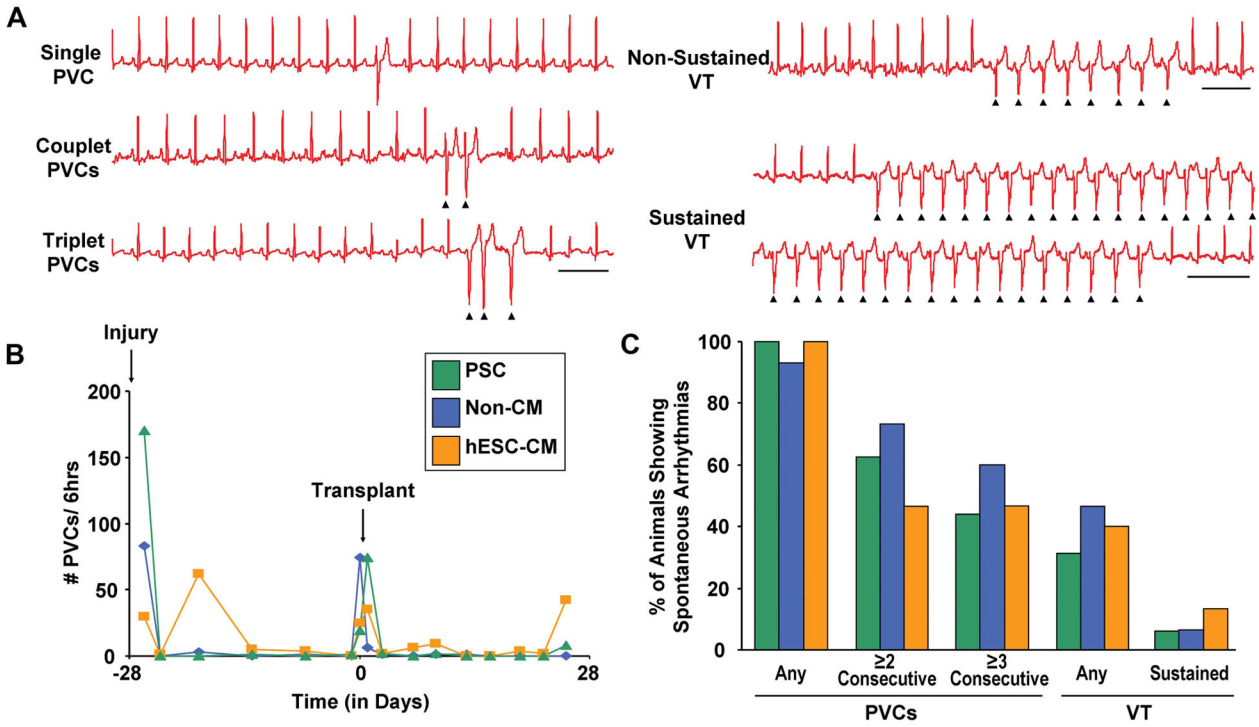

Figure 4. hESC-CM recipients and controls showed no difference in the incidence of spontaneous arrhythmias post-transplantation

Animals were monitored by telemetric ECG for spontaneous premature ventricular contractions (PVCs) and ventricular tachycardia (VT). **(A)** Representative episodes of single, couplet, and triplet PVCs, as well as non-sustained and sustained VT. Scale bars=500 ms. **(B)** Representative time-courses depicting the number of PVCs per hour in recipients of either pro-survival cocktail (PSC, green), non-cardiac hESC derivatives (blue, Non-CM) or hESC-CMs (orange). Note that all groups showed a spike in events associated with either cardiac cryoinjury (day −28) or cell transplantation (day 0). **(C)** Percentage of animals in each experimental group showing either PVCs (any or consecutive) or VT (any or sustained) during the monitoring period from day +3 to day +28 post-transplantation. No significant difference was detected between the three groups in terms of either the number of PVCs or VT per hour or in the percentage of animals exhibiting such events. (PSC, n=16. non-CMs, n=15. hESC-CMs, n=15.)

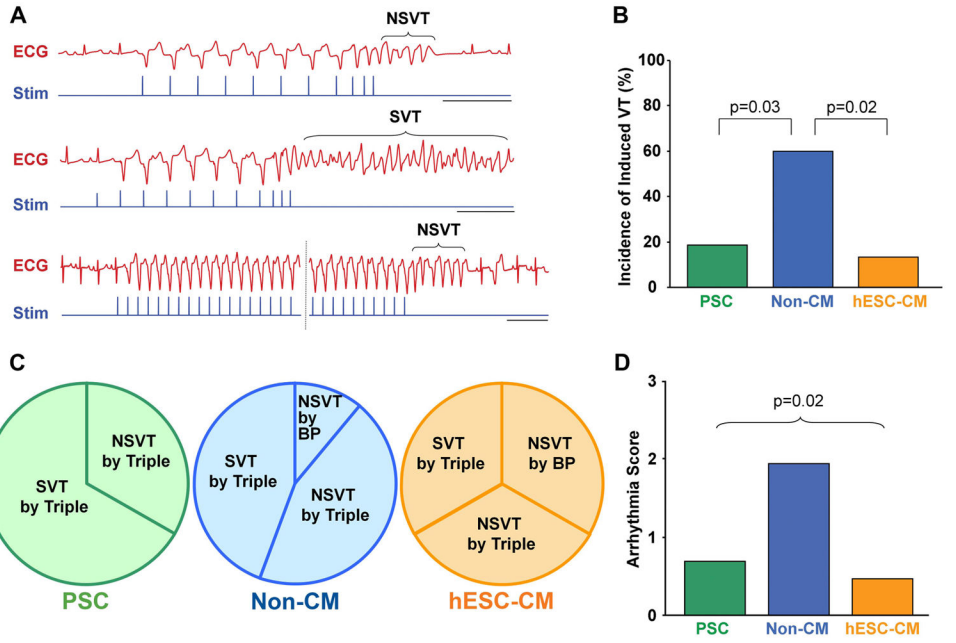

Figure 5. Recipients of non-cardiac hESC derivatives, but not hESC-CMs, showed a higher incidence of induced ventricular tachycardia

(A) Representative ECG traces (red) during programmed electrical stimulation (Stim, blue traces), performed on day +28 post-transplantation. The upper and middle pair of traces depict examples of non-sustained and sustained ventricular tachycardia (NSVT and SVT, respectively) induced by triple extra-stimuli. The lower pair of traces shows an episode of NSVT induced by burst pacing. Scale bars=500 ms. **(B)** Percentage of animals in each of the three experimental groups that showed any induced VT. Note that, while there was no significant difference between PSC (green) and hESC-CM (orange) recipients, animals receiving non-cardiac hESC-derivatives (Non-CM, blue) showed an ~3-fold greater incidence of induced VT. **(C)** For those animals belonging to each experimental group that were induced to VT, these pie-charts indicate the conditions required for induction (i.e. either triple extra-stimuli or burst pacing (BP)) and whether the animals exhibited non-sustained (NSVT) or sustained VT (SVT). **(D)** Mean semi-quantitative PES arrhythmia score for animals belonging to each experimental group. (PSC, n=16. non-CMs, n=15. hESC-CMs, n=15.)

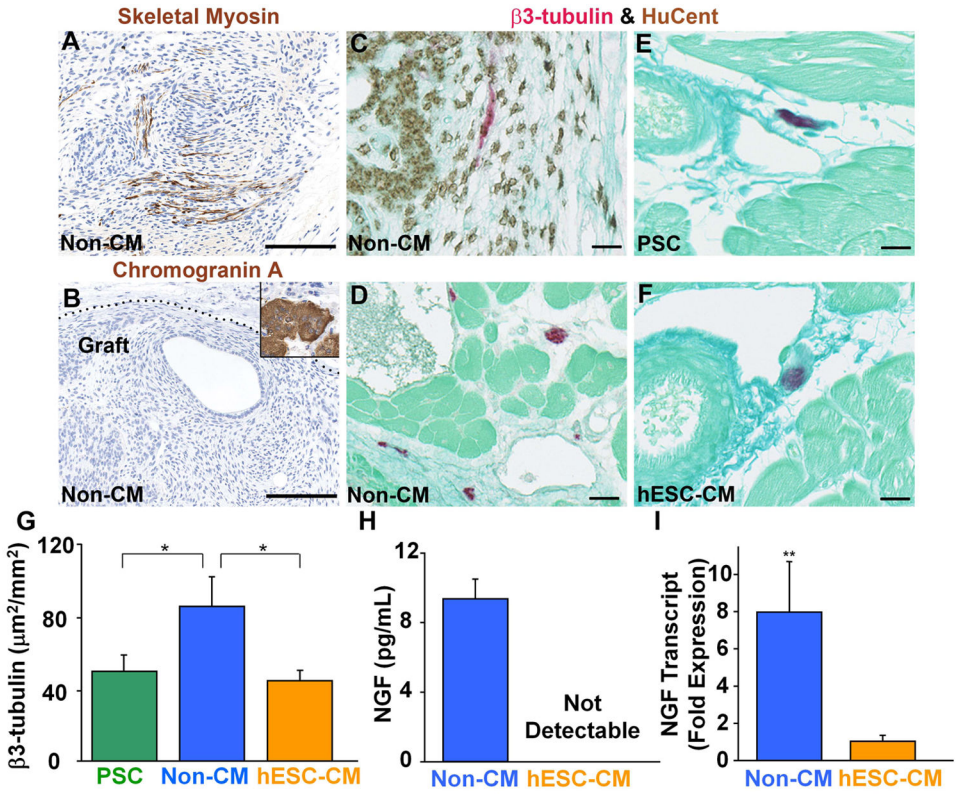

Figure 6. Other studies to explore the mechanistic basis for the electrical instability of non-cardiac cell recipients

(A–B) After identifying the graft cells by in situ hybridization with a human-specific probe on an adjacent histological section, grafts were further analyzed by immunostaining with antibodies against skeletal myosin **(A)** and chromogranin A **(B)**. The inset of panel B shows positive control staining on porcine pancreatic islet tissue. **(C–F)** Sections were double-stained by in situ hybridization for human-specific probe (brown) and immunohistochemistry for the neuronal marker β3-tubulin (red). The recipients of non-cardiac derivatives (non-CMs) showed very rare, double-positive graft-derived neuronal cells **(C)**. By contrast, we commonly observed single-positive host neurons in sections from recipients of non-CMs (D), PSC (E) or hESC-CMs (F). Scale bars=100 μm. **(G)** Mean cross-sectional area occupied by β3-tubulin-positive host neurons by experimental group. *P<0.05. **(H)** By ELISA assay, conditioned medium from non-CMs showed far greater levels of nerve growth factor (NGF) than that from hESC-CMs. ND=not detectable. n=3 per condition. **(I)** NGF transcript in non-CM versus hESC-MC cultures as determined by qRT-PCR. n=3 per condition.

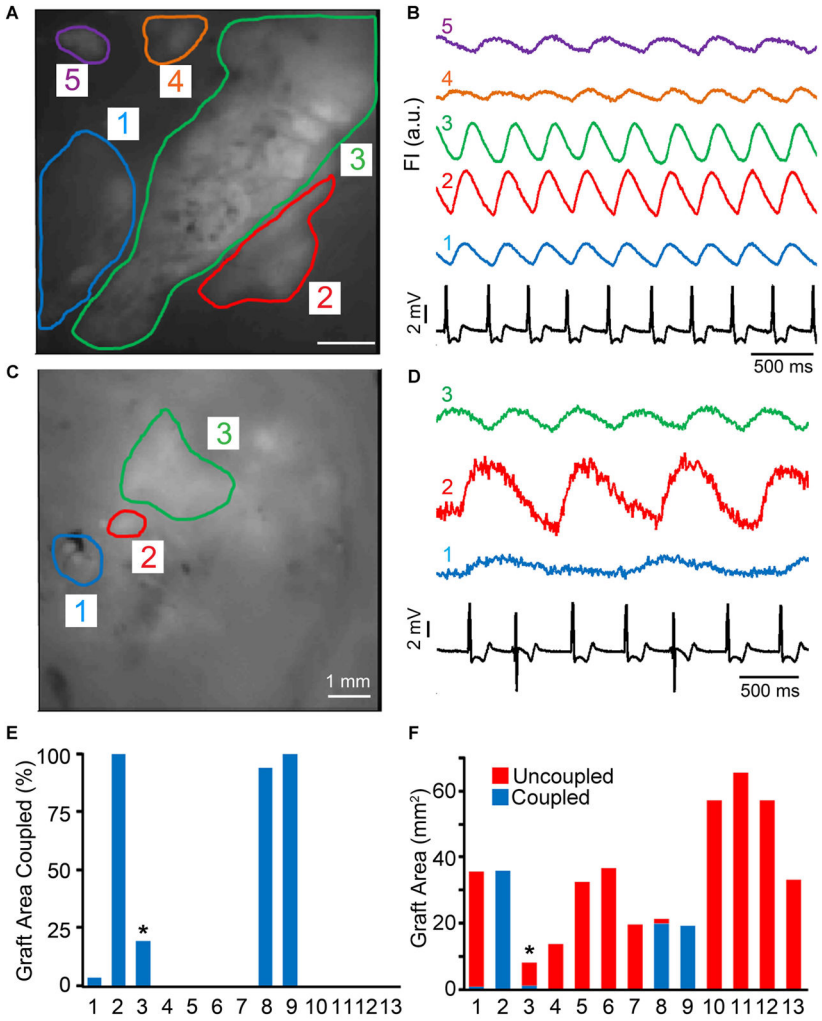

Figure 7. hESC-CM graft coupling in chronically cryoinjured guinea pig hearts

Intravital imaging of chronically injured hearts with GCaMP3+ hESC-CM grafts was performed at 14 days post-transplantation. **(A)** Still image of the epicardial surface of a representative heart with 5 separate regions of GCaMP3+ graft. **(B)** Corresponding GCaMP3 fluorescence traces over time for each region of interest (ROI), as well as the simultaneously host ECG (black trace). Note that transients in ROIs 1–4 occurred in a 1:1 relationship with QRS complexes of the host ECG, while uncoupled RO1 5 (purple) activated independently. **(C)** Still image from a different heart with three graft ROIs, all of which activated independently from the host ECG (**D**). **(E)** Percentage of the visible GCaMP3+ hESC-CM graft footprint in each of the 13 hearts analyzed that showed 1:1 coupling with the host ECG. The asterisk indicates the one heart in which all of the 1:1 coupled graft resided in healthy host myocardium adjacent to cryoinjury zone. The images depicted in panels **7A&B** were from heart #8. **(F)** Area of coupled (blue) and uncoupled (red) GCaMP3+ hESC-CM graft in each of the 13 hearts analyzed.